RESISTANCE OF WELDED TUBULAR T- AND X-JOINTS MADE OF HIGH STRENGTH STEEL AT ELEVATED TEMPERATURES

EMRE OZYURT[1,2] and YONG C. WANG[2]

[1]*Department of Civil Engineering, Gumushane University, Gumushane, Turkey.*
E-mail: emre.ozyurt@gumushane.edu.tr
[2]*School of Mechanical, Aerospace and Civil Engineering, Manchester University, Manchester, UK.*
E-mail: yong.wang@manchester.ac.uk

This study numerically examines the resistance of welded tubular T- and X-joints made of high strength steel (HSS) subjected to brace axial load or bending moment at elevated temperatures. After validation of the numerical simulation model, an extensive number of Finite Element simulations of tubular T- and X-joints at different elevated temperatures were performed using the non-linear finite element package ABAQUS v6.14-1. The numerical simulations covered a wide range of parameters, such as brace to chord diameter ratio, joint type, section type and loading condition.
In the authors' previous research on welded tubular joint resistance for normal strength steel T- and X-joints with the brace member in compression, the results indicated that the reduction in joint strength at elevated temperatures followed the steel Young's modulus reduction factor. This is because joint resistance under the failure mode of chord face plastification is related to chord face deformation which is governed by the Young's modulus of steel. However, for HSS, its yield strength decreases faster than its Young's modulus at elevated temperatures. The results of this study suggest that for HSS welded tubular joints at elevated temperatures, the yield strength reduction factor of HSS can be generally used to modify the ambient temperature joint resistance. This study confirms that the same trend is followed by different joint geometries and loading conditions.

Keywords: Design, Elevated temperature, Joint resistance, Tubular joints.

1 Introduction

Hollow sections have widely used in the structural applications, especially Circular Hollow Section (CHS) and Square/Rectangular Hollow Sections (SHS/RHS). High Strength Steel (HSS) has become popular recently, for large span constructions, offshore platforms, skyscrapers, etc. Using high strength enables weight of the structure to be reduced. In case of fire, the resistance of tubular joints significantly decreases as the mechanical properties of steel are deteriorated. Indeed, the resistance of welded tubular joints made of normal strength of steel may decrease even faster than the reduction in the yield strength at elevated temperatures. However, the degradation of mechanical properties of HSS at elevated temperatures differs from those of normal strength steel. Therefore, there is a need to examine the effects of deterioration of mechanical properties of HSS on welded tubular joint resistance at high temperatures.

A considerable amount of research has been published on HSS T- and X-joints at ambient temperature. These studies examine how to calculate HSS joint resistance using the design guide

Proceedings of the 17th International Symposium on Tubular Structures.
Editors: X.D. Qian and Y.S. Choo
Copyright © ISTS2019 Editors. All rights reserved.
Published by Research Publishing, Singapore.
ISBN: 978-981-11-0745-0; doi:10.3850/978-981-11-0745-0_032-cd

equations for normal strength steel, considering geometrical parameter, loading condition and section type (Fleischer et al., 2008, Puthli et al., 2010, Becque and Wilkinson, 2017, Mohan and Wilkinson, 2012, Cheng and Becque, 2016, Lee et al., 2017). To date, there is a paucity of evidence on the behavior of HSS T- and X-joints under fire conditions. However, there is no information in the current design guides, such as Eurocode EN 1993-1-8 (CEN, 2005) and the CIDECT design guides (Packer et al., 2009, Wardenier et al., 2008), for mechanical properties of HSS at elevated temperatures. Therefore, assumptions had to be made in this study focusing on joint resistance of HSS T- and X-joints under different loading conditions at elevated temperatures. The material properties in the parametric study were based on the elevated temperature test data for HSS of (Chen et al., 2006).

2 Verification Study

This study is based on assessment of numerical simulation results using the general finite element package ABAQUS/Standard v6.14-1. Since there is no available test data on welded tubular joints made of HSS in fire conditions, the test results of CHS X-joints made of S690 under brace axial compression (R32, 33 and R42) or tension (R29 and R41) or in-plane bending moment loads (R39 and R40-2) at ambient temperature (Puthli et al., 2010) were used for validation. The previous research studies of the authors on welded tubular joints made of normal strength steel at elevated temperatures (Ozyurt et al., 2014, Ozyurt and Wang, 2018) can be considered to validate the authors' numerical model for elevated temperature modeling.

Puthli et al. (2010) carried out tests on X-joints with brace member in compression or tension or in-plane bending. The geometrical details and material properties of specimens of Puthli et al. (2010) are summarized in Table 1. d and b refer to chord and brace diameters, f_y and f_u indicate yield stress and ultimate stress of steel and 0 and i subscripts indicate chord and brace members, respectively. The angle was 90° between the chord and brace members. The Young's modulus and ultimate strain were assumed to be 210 GPa and 10%, respectively.

Table 1. Geometrical parameters and mechanical properties of specimens of Puthli et al. (2010)

Specimen	Chord member				Brace members			
	d_0	b_0	f_{y0}	f_{u0}	d_i	b_i	f_{yi}	f_{ui}
R29,32	325.0	15.0	734	802	178.1	8.7	759	809
R33	325.1	19.1	739	798	178.1	8.5	727	793
R39	178.3	12.6	788	834	178.1	8.6	759	809
R40,42	177.8	8.4	727	793	178.0	8.6	727	793
R41	178.2	8.7	727	793	178.1	8.6	727	793

In the ABAQUS simulation model, the Riks method was chosen to apply axial loads in brace members. Bilinear material properties of steel were converted into true stress-strain as described by Boresi and Schmidt (2003). 20-noded solid quadratic (C3D20R) elements with reduced integration, with two elements in the thickness direction, were used for each member, including weld geometry. In order to save computational time, a quarter of the joint was used and boundary conditions at the symmetrical edges were appropriately applied based on the symmetrical planes. After mesh convergence study, the suitable mesh sizes in the intersection zone and away from the joint zone were chosen as a value of 10 mm and 20 mm, respectively.

Figure 1 illustrates a comparison of load-indentation curves of CHS X-joints under brace axial compression and in-plane bending between the test results of Puthli et al. (2010) and the authors' numerical simulations. It can be seen from Figure 1 that the results were excellent for CHS X-joints under axial brace compression. Although there is a slight difference for the joints under in-plane bending moments due to using bilinear material properties, the joint ultimate loads were very close to the test results.

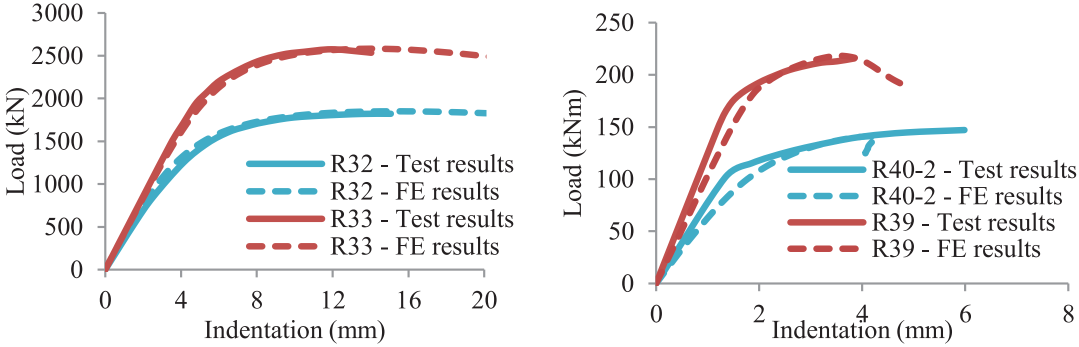

a) Under brace axial compression b) Under brace in-plane bending

Figure 1. Comparisons of load-indentation curves between the test and FE results

Figure 2 compares the deformed shapes of R32 joint between the test and FE results since this is the only available deformed shape picture in the test report. As can be seen from Figure 2, the failure was chord plastification and the deformed shapes were similar.

a) Test of Puthli et al. (2010) b) FE results

Figure 2. Comparison of deformed shape of R32 specimen between test and FE results

Table 2 compares the peak loads of the joints between the test results of Puthli et al. (2010) and the authors' numerical results, including the ratio of the test to numerical simulation results. Table 2 clearly shows that there is an excellent agreement between the test and FE results.

Table 2. Comparison of joint resistances between the test and numerical results

Specimen	Test Results	FE results	Ratio of the FE to test results
R29-T	1890 kN	1788 kN	0.94
R32-C	1770 kN	1850 kN	1.04
R33-C	2520 kN	2582 kN	1.02
R39-IB	225 kNm	218 kNm	0.97
R40-2-IB	140 kNm	141 kNm	1.01
R41-T	1995 kN	1929 kN	0.97
R42-C	1567 kN	1502 kN	0.96

This validation study clearly confirms that the behavior of welded tubular joints made of HSS can be successfully simulated. The previous experience of the authors on welded tubular joints made of normal strength of steel at high temperatures can be combined with the further validation exercise of this paper to give confidence in using the authors' simulation model to examine HSS tubular joints at elevated temperatures.

3 Parametric Study and Results

3.1 *Detail of parametric study*

An extensive number of HSS tubular joints were simulated at different temperature levels, considering the joint type (T- and X-joints), different loading case (axial brace compression, axial brace tension, in-plane bending moment and out-of-plane bending moment), the section type (CHS or SHS) and brace-to-chord diameter ratio (β). The chord diameter/width of all CHS and SHS joints were taken to be 244.5 mm and 250 mm, respectively, with the wall thickness for both the brace and chord members being 8 mm. The nondimensional geometrical parameter β ranged between 0.47 and 1. The temperature distribution was assumed to be uniform for both the chord and brace members. Each joint was analyzed at 20 °C, 500 °C, 600 °C, 700 °C, and 800 °C.

The mechanical properties of HSS at elevated temperatures were based on the test results of Chen et al. (2006). S690Q steel was used in their coupon tests which had stress at 2% strain of 823 MPa and a modulus of elasticity of 223 GPa at room temperature. They carried out transient-state condition tests. Table 3 gives their test results of reduction factors for yield strength (2% strain) and Young's modulus.

Table 3. Reduction factors of Young's modulus and yield strength of HSS (Chen et al., 2006)

Temperature (°C)	Elastic Modulus (GPa)	Yield Strength (2% strain) (MPa)	$k_{E,\theta}$	$k_{y,\theta}$
22	223000	823.00	1.00	1.00
60	231920	790.08	1.04	0.96
120	225230	831.23	1.01	0.96
150	231920	814.77	1.04	0.99
180	227460	798.31	1.02	0.97
240	218540	823.00	0.98	1.00
300	220770	814.77	0.99	0.99
410	205160	773.62	0.92	0.94
460	209620	691.32	0.94	0.84
540	194010	609.02	0.87	0.74
600	162790	485.57	0.73	0.59
660	162790	345.66	0.73	0.42
720	113730	181.06	0.51	0.22
770	109270	115.22	0.49	0.14
830	73590	74.07	0.33	0.09

For all numerical models, the chord length was chosen as 2500 mm, which was 10 times the diameter of the chord member as suggested by Vegte et al. (2010), in order to eliminate the effects of boundary conditions and chord length. All degrees of freedom at the chord member ends were restricted.

3.2 *Definition of joint resistance*

In the case of normal strength steel, load resistance of welded hollow section joints under brace axial load was based on the deformation limit of Lu et al. (1994). The joint resistance was defined by the peak load or the load at 3% indentation at the intersection area of chord face in the load-indentation curve. For tubular joints with bending moment in the brace member, the joint resistance was determined by the deformation limit of Yura et al. (1980). In this case, the joint resistance was equal to the peak load or the load at $80f_y/E$ rotation of the brace member in the moment-rotation curve. These definitions may not be safe for tubular joints made of HSS, because tensile membrane action can occur before the deformation limit of Lu et al. (1994) and Yura et al. (1980).

Figure 3 illustrates typical load-indentation curves of CHS joints under brace compression load at various temperatures, including the deformation limit of Lu et al. (1994). The peak load occurred well before the deformation limit in each case. In addition, there was no development of tensile membrane action (which would be shown as increasing load after an initial peak). The same trends are observed in other joints under brace axial load. Therefore, in this research, the peak load is taken as the joint resistance for joints under brace axial load.

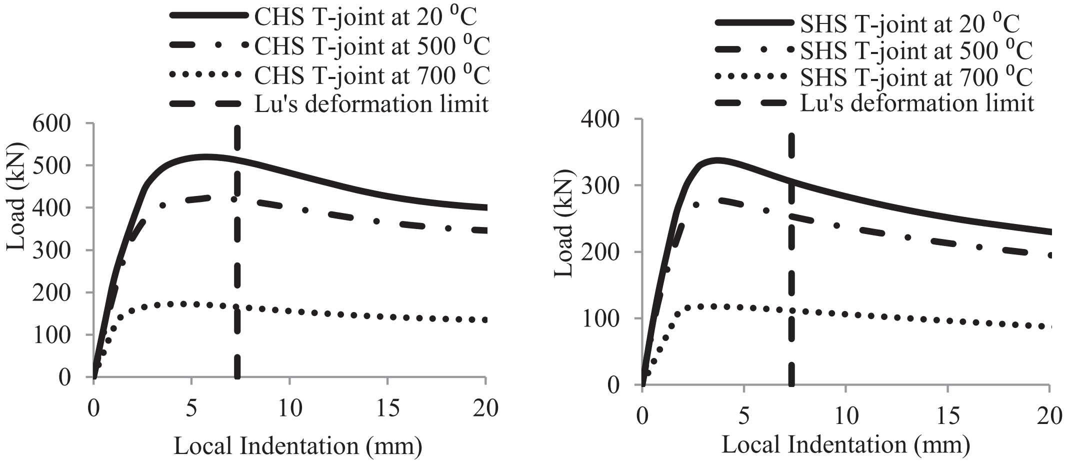

a) CHS T-joint (β=0.47) b) SHS T-joint (β=0.47)

Figure 3. Load-ovalization curves of CHS T-joints under brace axial compression at ambient and elevated temperatures

When the brace member was subjected to bending moment, tensile membrane action was able to develop before reaching Yura's deformation limit as illustrated in Figure 4. However, using the load at Yura's deformation limit may not be safe for HSS T- and X-joints with brace in bending. Therefore, the alternative criterion of twice elastic slop (TES), based on Rao (2002) was used. In this definition, the joint resistance, for tubular joints with brace bending moment, is the moment corresponding to the intersection of twice the slope of the initial elastic line and the moment-rotation curve. Figure 4 illustrates typical moment-rotation curves of CHS T-joints under brace out-of-plane bending moment, including both Yura's deformation limit and TES lines. The TES limit is used for other joints under brace bending.

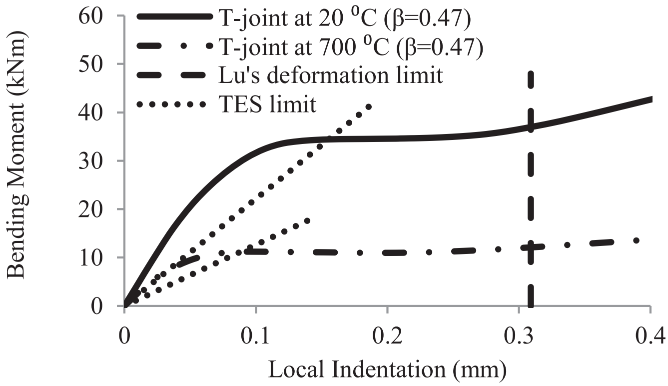

Figure 4. Moment-rotation curves of CHS T-joints under out-of-plane bending moment

3.3 *Effect of brace axial load*

This section investigates the variation of joint resistance at elevated temperatures under brace axial load. The joint resistance is normalized to that at ambient temperature by presenting the ratio of joint resistance at elevated temperature to that at ambient temperature.

Figure 5 compares joint resistance ratios at different temperatures with reduction factors for yield strength and Young's modulus of HSS from the test results of Chen et al. (2006). In all cases, the joint resistance ratios follow steel yield strength reduction factors. This is in contrast with joints with normal strength steel. In joints with normal strength steel, the Young's modulus reduction factor is lower than the yield strength reduction factor. Due to second-order effects as a result of large chord deformation, the joint strength was dominated by the effects of changing Young's modulus. In joints of HSS, due to higher retention of Young's modulus at elevated temperatures, the chord deformations were low and the second order effects disappear. Therefore, the variation of joint resistance at elevated temperatures follows that of HSS yield strength.

Under brace member tensile load, there is no second order effect in either normal strength steel or HSS joints, therefore, the variation of joint resistance follows that of HSS yield strength reduction factor at elevated temperatures. The above trend was found to be independent of joint type, section type and β value as shown in the scatter data in Figure 5.

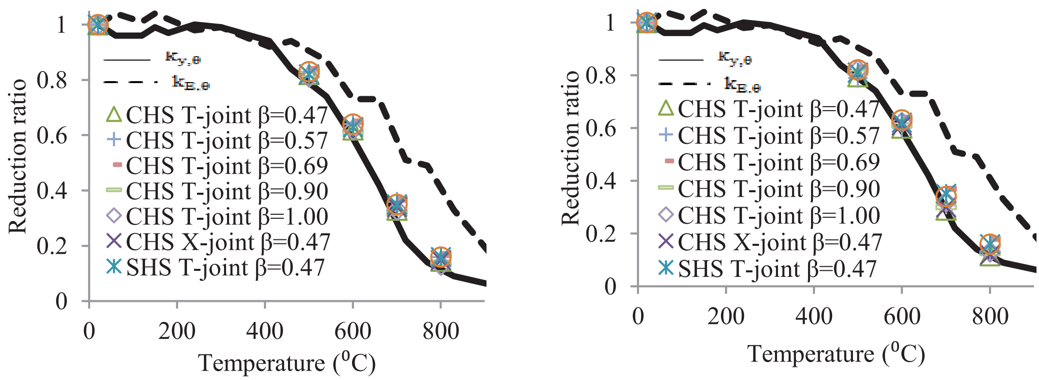

a) Axial compression load in brace member b) Axial tension load in brace member

Figure 5. Comparison of elevated temperature resistance ratios of HSS tubular joints

3.3 *Effect of brace bending moment*

Figure 6(a) and (b) present results for HSS T- and X-joints with brace member under either in-plane bending or out-of-plane bending, respectively. As with the results for brace member under axial load, the results in Figure 6 confirm that reductions in joint resistance at elevated temperatures follow those of the yield strength of HSS.

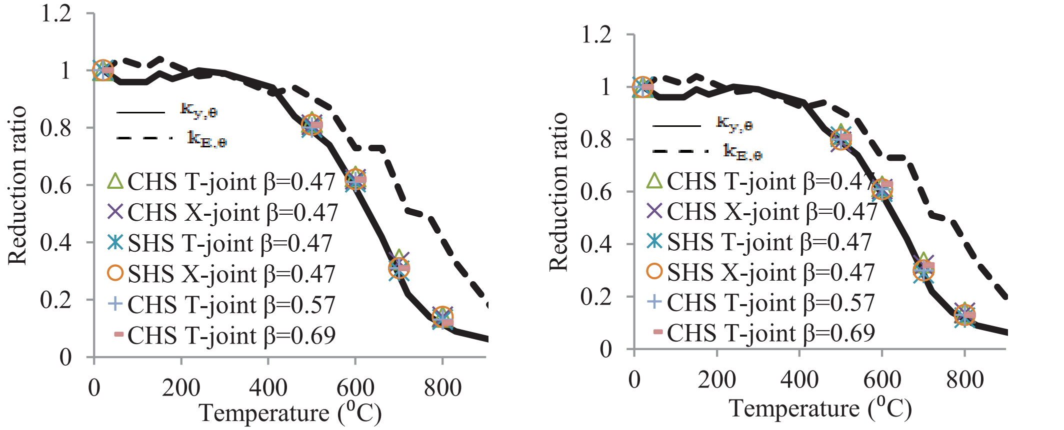

a) In-plane bending moment in brace member b) Out-of-plane bending moment in brace member

Figure 6. Comparison of elevated temperature resistance ratios of HSS tubular joints under brace bending moment

3 Conclusions

A numerical investigation was carried out in this study to evaluate variations of resistance of welded tubular T- and X-joints made of HSS subjected to brace axial load or bending moment at elevated temperatures. After validation of the numerical simulation model, an extensive number of Finite Element simulations of tubular T- and X-joints at different elevated temperatures were performed using the mechanical properties of HSS at elevated temperature of Chen et al. (2006). Based on the numerical simulation results, it can be concluded that:

(i) When the brace member was under axial load, the peak load can be taken as joint resistance because this happened before joint indentation reached the deformation limit of Lu et al. (1994). For HSS joints under bending, the TES criterion was more appropriate to define as deformation limit of Yura et al. (1980) could result in unsafe results.

(ii) Contrary to T- and X-joints made of normal strength of steel with brace member under compression, the reduction in joint resistance followed the HSS yield strength reduction factor at elevated temperatures because HSS yield strength decreases more than HSS Young's modulus at elevated temperatures.

(iii) HSS T-and X-joint resistances under axial load or bending moment at elevated temperatures can be calculated by multiplying the ambient temperature resistances by the HSS yield strength steel reduction factor at elevated temperatures. This conclusion applies to any joint type, tubular section type and brace loading condition.

Acknowledgments

This research is supported by the Scientific and Technological Research Council of Turkey (TUBITAK-BIDEB, 2219 International Post-Doctoral Research Fellowship Programme). The authors would also like to acknowledge partial funding by CIDECT through its project 15U-7/18 Joints at high temperatures.

References

Becque, J. and Wilkinson, T., The capacity of grade C450 cold-formed rectangular hollow section T and X connections: An experimental investigation, *Journal of Constructional Steel Research*, 133, 345-359, 2017.

Boresi, A. P. and Schmidt, R., J., Advanced mechanics of materials, *John Wiley and Sons*, 2003.

CEN. Design of Steel Structures. In: PART: EN 1993-1-8-Design of Joints. London: Brussels, Belgium, 2005.

Chen, J., Young, B. and Uy, B., Behavior of high strength structural steel at elevated temperatures, *Journal of structural engineering*, 132, 1948-1954, 2006.

Cheng, S. and Becque, J., A design methodology for side wall failure of RHS truss X-joints accounting for compressive chord pre-load, *Engineering Structures*, 126, 689-702, 2016.

Fleischer, O., Herion, S. and Puthli, R., Numerical investigations on the static behaviour of CHS X-joints made of high strength steels, *Proc. 12th International Symposium on Tubular Structures*, 2008.

Lee, C.-H., Kim, S.-H., Chung, D.-H., Kim, D.-K. and Kim, J.-W., Experimental and numerical study of cold-formed high-strength steel CHS X-joints, *Journal of Structural Engineering*, 143, 04017077, 2017.

Lu, L. H., De Winkel, G. D., Yu, Y. and Wardenier, J., Deformation limit for the ultimate strength of hollow section joints, *Proceedings of the Sixth International Symposium on Tubular Structures*, Melbourne, Australia, 1994.

Mohan, M. and Wilkinson, T., FEA of T & X joints in Grade C450 steel, *Proceedings of the 14th International Symposium on Tubular Structures*, London, 185-194, 2012.

Ozyurt, E. and Wang, Y., Resistance of Axially Loaded T-and X-Joints of Elliptical Hollow Sections at Elevated Temperatures–A Finite Element Study. *Structures*, 15-31, 2018.

Ozyurt, E., Wang, Y. and Tan, K., Elevated temperature resistance of welded tubular joints under axial load in the brace member, *Engineering Structures*, 59, 574-586, 2014.

Packer, J. A., Wardenier, J., Zhao, X.-L., van der Vegte, G. J. and Kurobane, Y., Design guide for rectangular hollow section (RHS) joints under predominantly static loading, *CIDECT*, Verlag TUV Rheinland, Germany, 2009.

Puthli, R., Bucak, O., Herion, S., Fleischer, O., Fischl, A. and Josat, O., Adaption and extension of the valid design formulae for joints made of high strength steels up to S690 for cold-formed and hot-rolled sections, *CIDECT Project 5BT*, CIDECT, 2010.

Rao, K., Companion Guide to the ASME Boiler and Pressure Vessel Code: Criteria and Commentary on Select Aspects of the ASME Boiler & Pressure Vessel and Piping Codes, *ASME Press*, New York, 2002.

van der Vegte, G. and Makino, Y., Further research on chord length and boundary conditions of CHS T-and X-joints, *Advanced Steel Construction*, 6, 879-890, 2010.

Wardenier, J., Kurobane, Y., Packer, J., van der Vegte, G. J. and Zhao, X., Design guide for circular hollow section (CHS) joint under predominantly static loading, *Verlag TUV Rheinland*, Germany, Cidect, 2008.

Yura, J., Zettlemoyer, N. and Edwards, I., Ultimate capacity equations for tubular joints, *Offshore Technology Conference*, 1980.